Available online at www.sciencedirect.com
ScienceDirect
Advances in Space Research 41 (2008) 1666–1676
ADVANCES IN SPACE RESEARCH (a COSPAR publication)
www.elsevier.com/locate/asr

Furthering our understanding of electrostatic solitary waves through Cluster multispacecraft observations and theory

J.S. Pickett [a,*], L.-J. Chen [b], R.L. Mutel [a], I.W. Christopher [a], O. Santolík [a,c], G.S. Lakhina [d], S.V. Singh [d], R.V. Reddy [d], D.A. Gurnett [a], B.T. Tsurutani [e], E. Lucek [f], B. Lavraud [g]

[a] Department of Physics and Astronomy, The University of Iowa, Iowa City, IA 52242, USA
[b] Space Science Center, University of New Hampshire, Durham, NH 03824, USA
[c] Charles University, Faculty of Mathematics and Physics, Prague, and IAP/CAS, Prague 18000, Czech Republic
[d] Indian Institute of Geomagnetism, New Panvel (W), Navi Mumbai 410 218, India
[e] Jet Propulsion Laboratory, California Institute of Technology, Pasadena, CA 91109, USA
[f] The Blackett Laboratory, Imperial College, London SW7 2BZ, UK
[g] ISR-1, Space and Atmospheric Science, Los Alamos National Laboratory, Los Alamos, NM 87545, USA

Received 22 November 2006; received in revised form 6 May 2007; accepted 18 May 2007

Abstract

Nonlinear isolated electrostatic solitary waves (ESWs) are observed routinely at many of Earth's major boundaries by the Wideband Data (WBD) plasma wave receivers that are mounted on the four Cluster satellites. The current study discusses two aspects of ESWs: their characteristics in the magnetosheath, and their propagation in the magnetosheath and in the auroral acceleration (upward current) region. The characteristics (amplitude and time duration) of ESWs detected in the magnetosheath are presented for one case in which special mutual impedance tests were conducted allowing for the determination of the density and temperature of the hot and cold electrons. These electron parameters, together with those from the ion experiment, were used as inputs to an electron acoustic soliton model as a consideration for the generation of the observed ESWs. The results from this model showed that negative potential ESWs of a few Debye lengths (10–50 m) could be generated in this plasma. Other models of ESW generation are discussed, including beam instabilities and spontaneous generation out of turbulence. The results of two types of ESW propagation (in situ and remote sensing) studies are also presented. The first involves the propagation of bipolar type ESWs from one Cluster spacecraft to another in the magnetosheath, thus obtaining the velocity and size of the solitary structures. The structures were found to be very flat, with large scale perpendicular to the magnetic field (>40 km) and small scale parallel to the field (<1 km). These results were then discussed in terms of various models which predict such flat structures to be generated. The second type of propagation study uses striated Auroral Kilometric Radiation (SAKR) bursts, observed on multiple Cluster satellites, as tracers of ion solitary waves in the upward current region. The results of all studies discussed here (pulse characteristics and ESW velocity, lifetime, and size) are compared to in situ measurements previously made on one spacecraft and to theoretical predictions for these quantities, where available. The primary conclusion drawn from the propagation studies is that the multiple spacecraft technique allows us to better assess the stability (lifetime) of ESWs, which can be as large as a few seconds, than can be achieved with single satellites.

Keywords: Electrostatic solitary waves; ESW propagation; Cluster; Magnetosheath; Auroral acceleration region

1. Introduction

Electrostatic solitary waves (ESWs) have gained considerable attention in the last several years due to the introduction of plasma wave receivers that make high time resolution waveform measurements and due to the realiza-

* Corresponding author. Tel.: +1 319 335 1897; fax: +1 319 335 1753.
E-mail address: pickett@uiowa.edu (J.S. Pickett).

0273-1177/$34.00
doi:10.1016/j.asr.2007.05.064

tion that ESWs are observed in almost every boundary layer and turbulent region of space where satellite measurements have been made. ESWs are isolated pulses observed in the electric field waveform data and can be of several types: bipolar (two half sinusoids of opposite polarity), tripolar (two half sinusoids of one polarity with an intervening half sinusoid of opposite polarity and with the central pulse generally having a larger amplitude than the two outer pulses), offset bipolar (a bipolar with an extended, nearly null field separating the two oppositely directed half sinusoids), and unipolar (one half sinusoid). A recent review of many of the observational and theoretical results, which relate primarily to Earth and its environs, can be found in Tsurutani et al. (1998), Lakhina et al. (2000), Franz et al. (2005), and Chen et al. (2005). In addition, Williams et al. (2005, 2006) discuss the observations of ESWs during an interplanetary shock crossing at 8.7 a.u. and in the vicinity of Saturn's magnetosphere, respectively. All of these observations and the theoretical studies that reference them have led to the conclusion that most of the ESWs represent potential structures, primarily electron and ion phase space holes, but also possibly density enhancements and compressions, and weak double layers. The mechanism responsible for the generation of the ESWs, their characteristics and their effect on the ongoing plasma processes have also been widely discussed in the many references provided in Lakhina et al. (2000), Franz et al. (2005), and Chen et al. (2005).

Most of the observations that have been reported thus far are from a single spacecraft, some of them configured in an interferometry mode in order to obtain ESW velocity and size by measuring the time delay of detection of the ESW on one antenna to detection of it on another antenna on the same spacecraft. The Cluster spacecraft are providing new insights into ESW characteristics and propagation through the multispacecraft aspect of the mission (observing ESW propagation from one spacecraft to another) as well as through the high time resolution, larger bandwidth measurements afforded by the Wideband Data (WBD) plasma wave receiver (Gurnett et al., 1997). The WBD instrument makes extremely high time resolution waveform measurements, as high as 4.5 μs, over wide frequency bandwidths as detailed in Pickett et al. (2003).

The bulk of the theory and simulation studies so far have concentrated on trying to understand observations made in the auroral acceleration region. Thus, there is much to be learned by applying the various theories for generation of ESWs, such as through beam and acoustic instabilities, to the observational data reported in all the other regions where it is more likely the case that the electron plasma frequency is higher than the electron cyclotron frequency. One region that is particularly rich in ESWs, the magnetosheath, has only recently been studied in detail observationally with regard to ESWs by Pickett et al. (2003, 2005) using Cluster WBD data. Most of the ESWs observed in this region as reported by Pickett et al. (2003, 2005) have extremely short time durations (~100 μs or less). These short time duration ESWs observed in the magnetosheath have most likely not been reported in the literature before these Cluster observations due to limitations of the hardware (waveform receivers with insufficient bandwidth and/or sampling rate) or spacecraft with sufficient hardware that do not encounter the magnetosheath.

Below we report on some recent observations of ESWs made by Cluster WBD in the magnetosheath, obtaining their characteristics and discussing various generation mechanisms for this region. This is followed by a propagation study that relies on multiple Cluster satellite observations to determine propagation characteristics. The propagation study consists of two parts: (1) ESW propagation observed in situ in the magnetosheath, and (2) ESW propagation in the auroral acceleration region observed remotely. We complete our study with a summary of ESW characteristics, including an assessment of their lifetime, and the conclusions to be drawn from these results.

2. Magnetosheath ESW characteristics

2.1. Observations

ESWs are almost always observed in Earth's dayside magnetosheath as the Cluster spacecraft traverse this highly turbulent region (see e.g., Pickett et al., 2003, 2005). The time durations of the ESW pulses observed in the magnetosheath are usually the smallest of those found anywhere in the Cluster orbit (see Figs. 3(b) and 4(b) of Pickett et al., 2004a), being on the order of a few tens to a few hundred μs. An example of some typical bipolar ESW pulses observed on 11 April 2004 on Cluster Spacecraft 4 (SC4) is shown in panel a of Fig. 1. This panel shows the electric field, in mV/m, plotted on the vertical axis, vs. time, in seconds since 00:46:35.923 UT, plotted on the horizontal axis, covering a 3 ms time period. In this figure we have pointed out two bipolar pulses that our automatic detection algorithm (see Pickett et al., 2004a) picked out as fitting our strict criteria for being isolated, having non-clipped amplitudes, being nearly symmetrically formed about the zero field level, and falling well within the frequency constraints for pulses that will not be distorted by the analog filters used in the WBD instrument. Their fields are very small, being on the order of 0.1 mV/m peak-to-peak. During this time, the angle of the receiving antenna to the background magnetic field was about 60°. Note that the identified pulses have time durations around 75 μs, and that all the pulses in this time period appear to have similar time durations and the same polarity (initial pulse negative). In the magnetosheath, however, WBD often observes opposite initial polarities throughout small samples of data, thus implying that the ESWs are either of opposite polarity or traveling in opposite directions, which is significant because this is often not the case in other regions of the magnetosphere where ESWs are observed. Because of hardware limitations, though, WBD is unable to determine whether the electric field associated

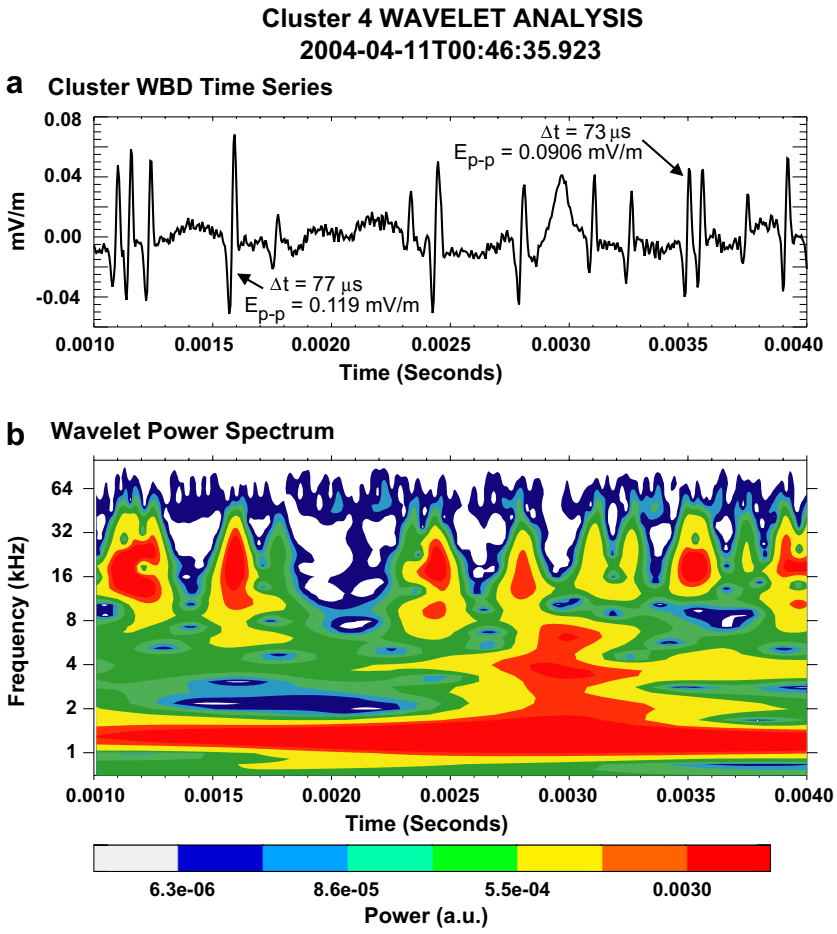

Fig. 1. Typical electrostatic solitary waves observed in the magnetosheath: (a) WBD waveform measurements showing a series of small amplitude, very short time duration bipolar pulses all of the same polarity, and (b) wavelet power spectrum of the waveforms from panel a showing the ESWs localized in time and frequency (around 16 kHz).

with any specific ESW is pointing earthward or anti-earthward using the polarity of the initial pulse as a basis.

In panel b of Fig. 1 we have provided the wavelet power spectrum with frequency, in kHz, plotted on the vertical axis, vs. time, in seconds since 00:46:35.923 UT, plotted on the horizontal axis, and color representing power, in arbitrary units (a.u.) related to the measured electric field, according to the color bar shown beneath the spectrogram. We have used a Morlet wavelet to carry out our wavelet analysis. The wavelet transform provides a time–frequency localization that is scale independent, unlike a Fourier transform. Here we can clearly see that the pulses are centered on a frequency of about 16 kHz, which is consistent with their time durations being less than 100 μs. Also through the use of the wavelet transform we can observe that the ESWs are localized in time and frequency.

In order to see a slightly larger picture of the distribution of ESWs in time, we have run our ESW detection software for the period 00:42 to 01:02 UT on 11 April 2004, which encompasses the time period presented in Fig. 1. Fig. 2 is a two panel plot covering this extended period of time throughout which SC4 was in the dayside magnetosheath at about 11.5 R_E, 17.7 λ_M (geomagnetic latitude) and 09:39 MLT (magnetic local time). Both panels (a) and (b) have time, in UT, plotted on the horizontal axis, while panel (a) has the measured peak-to-peak electric field, in mV/m, and panel (b) the pulse time duration, in ms, plotted on the left horizontal axes, respectively, for bipolar ESW pulses (black dots) that were automatically detected in the waveform data. The solid black line in both panels represents the magnetic field strength, in nT, according to the scale given on the right vertical axes measured by the FGM instrument (Balogh et al., 1997). Here we can see that the magnetic field shows significant variations throughout this 20-min period. The ESWs were detected continuously throughout this time period with time durations on the order of 40–250 μs, which is the upper limit for avoiding waveform distortion for this WBD mode, and with amplitudes varying from about 0.03 to 0.6 mV/m. We have also associated the times of ESW wave detections with the angle of the receiving antenna to the background magnetic field. A histogram showing the occurrence probability (vertical axis) vs. the antenna angle (horizontal axis) is shown in Fig. 3. It would appear that at least for this period of time, there is a preference for this angle to be around 50° or 110–140° to the magnetic field, i.e., very

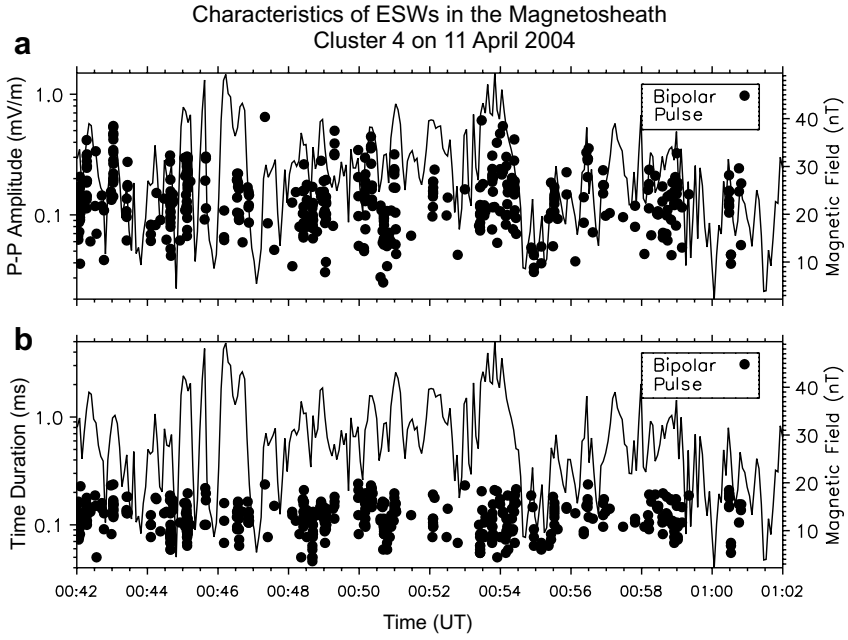

Fig. 2. Bipolar ESWs (black dots) detected in the magnetosheath over a 20 min period: (a) peak-to-peak electric field, and (b) pulse time duration. The solid black line is the measured magnetic field according to the scale shown on the right vertical axis. ESWs are detected throughout this interval with the exception of times when the magnetic field is low (<10 nT).

oblique, and not strictly parallel or perpendicular. This, and the fact the bipolar pulses are nearly symmetrically shaped as shown in the example in Fig. 1(a), may imply that these ESWs are not propagating strictly along the magnetic field as is often the case with ESWs observed elsewhere around Earth. However, the antenna angle (to **B**) occurrence, irrespective of ESW detection, goes as $\sin(\theta)$. Thus, the results shown in Fig. 3 do not discount the possibility that the ESWs are propagating along the magnetic field. The ESWs will still be symmetrically shaped when detected at angles other than at 0° or 180°, but have larger amplitudes than what are measured. Since WBD makes a measurement along one axis only, it is not possible to transform the measurements to a field-aligned coordinate system, which is why we must resort to investigating the total angle of the electric antenna (that WBD is using) to the magnetic field.

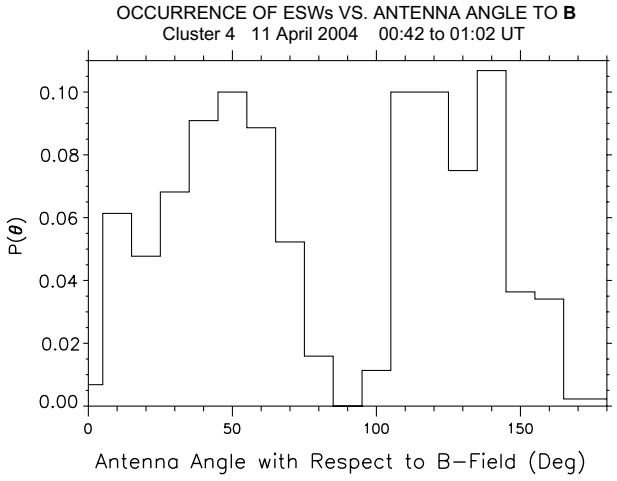

Fig. 3. Histogram of the occurrence probability of detected ESWs vs. the angle of the electric field antenna to the measured magnetic field for the 20 min period shown in Fig. 2. For this case, most ESWs are detected when the antenna is at large angles to the magnetic field.

2.2. Theory and modeling of ESW characteristics

We have chosen this particular magnetosheath event of 11 April 2004 because special mutual impedance tests were being carried out by the Whisper sounder on the other three Cluster spacecraft (SC1, SC2, SC3), but most intensely on SC1. At this time the spacecraft separations were on the order of 300 km. Thus, the plasma environments of all of them are very similar. The results of these tests are provided in Béghin et al. (2005). The tests provided the means, through modeling of the antenna response, to determine the electron density and temperature from the mutual impedance test data obtained on SC1. The analysis of the test data and the antenna modeling for the period 00:46–00:47 UT (a period which encompasses the waveform measurements shown in Fig. 1) showed that there were two electron components present with the following characteristics: $n_c \sim 16\ \mathrm{cm}^{-3}$, $T_c \sim 39\ \mathrm{eV}$, $n_h \sim 8\ \mathrm{cm}^{-3}$, and $T_h \sim 79\ \mathrm{eV}$ with $\lambda_D \sim 11\ \mathrm{m}$, where λ_D is the Debye length based on the hot electron temperature and total electron density. These results were in good agreement with the measured electron distribution function (see Fig. 9 of Béghin et al., 2005) which shows a typical measured flat topped distribution. As deduced from the zero-order moment of the distribution function, the electron density from the

PEACE (Johnstone et al., 1997) data was found to be about 24–25 cm^{-3} with an average of 38–39 eV for the parallel and perpendicular temperatures. Thus, the total electron density obtained by PEACE agrees very well with the density obtained from the active mutual impedance experiment with the measured electron temperature being that of the major constituent derived from the two-component model. For this same time period we also analyzed the ion data from the CIS instrument (Rème et al., 2001) on Cluster SC3, which are indicative of the ion environment of all four spacecraft because of the close separations. We obtained values of $n_i \sim 20\ cm^{-3}$ and $T_i \sim 200$ eV.

These electron and ion data were then input to a model consisting of unmagnetized plasma with hot electrons obeying the Boltzmann distribution, fluid cold electrons and ions. The model is a simple 1D model for electron acoustic solitons using the Sagdeev pseudo-potential technique (Singh et al., 2001; Singh and Lakhina, 2004). Our results are shown in Fig. 4. Plot (a) of this figure shows the Sagdeev potential, $V(f)$, on the vertical axis vs. the normalized potential, f, on the horizontal axis for three different values of the acoustic Mach number, M, which is the velocity of the structures normalized to the hot electron thermal velocity. For the input parameters outlined in the previous paragraph, the range of Mach numbers over which electron acoustic solitons were observed was 1.407–1.474. This corresponds to soliton velocities close to, but slightly higher than, the phase velocity of electron acoustic waves. This plot shows that only negative potential structures (compressions of the cold electron density) are formed and that they are propagating at speeds around the electron acoustic velocity, as opposed to the much slower ion acoustic speeds. Plot (b) shows the normalized potential amplitude, f, on the vertical axis vs. the size, X, on the horizontal axis of the electron acoustic solitons for the same three values of the acoustic Mach number. This plot shows us that as the amplitude of the solitons decreases the size increases. In summary, only negative potential electron acoustic solitons are admitted by the electron acoustic mode given these input conditions of the magnetosheath resulting in typical normalized soliton potential amplitudes of 0.01–0.03 and typical soliton widths of 1–5 Debye lengths ($\approx$ 10–50 m).

It is difficult to compare the electron acoustic soliton model results to the measurements. Although this model shows that electron acoustic solitons may be generated in the magnetosheath plasma, we are unable to say definitively that the ESWs that are measured by WBD are electron acoustic modes. First, WBD is unable to determine whether the measured ESWs are positive or negative potential or whether they are one or multi dimensional because it measures the average potential between the two electric field spheres along one axis only. Second, WBD is unable to determine the velocity of the structures since it cannot employ an interferometry type mode to do this on one spacecraft, or measure the propagation from one spacecraft to another for this case. Thus, we must make further refinements to the model, such as incorporating electron beams if present which would then allow for positive potential structures (rarefactions in cold electron density)

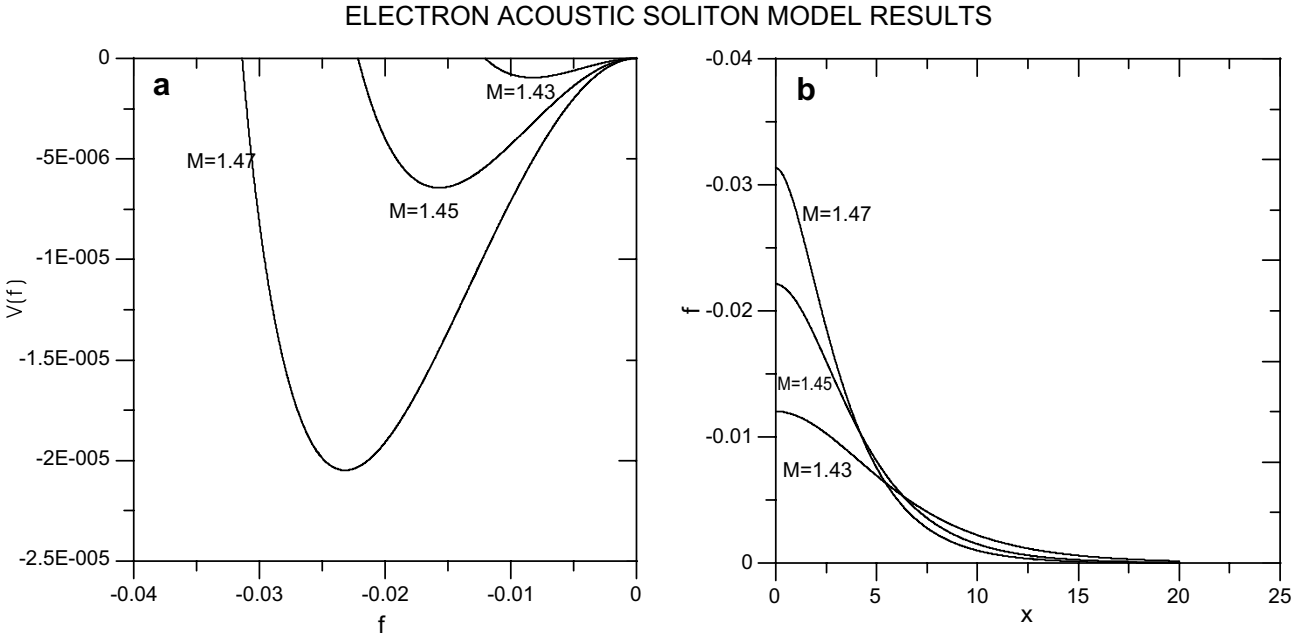

Fig. 4. Results from electron acoustic soliton model for the time period shown in Fig. 1: (a) Sagdeev potential vs. the normalized potential for three values of the acoustic Mach number (normalized to the hot electron thermal velocity), and (b) normalized potential amplitude vs. the soliton size for the same three Mach numbers. Only negative potential solitons (compression in cold electron density) are generated. The data used in the calculations are cold electron density and temperature, $n_c \sim 16\ cm^{-3}$ and $T_c \sim 39$ eV, and hot electron density and temperature, $n_h \sim 8\ cm^{-3}$ and $T_h \sim 79$ eV, respectively. The ion temperature was taken as $T_i = 200$ eV.

in certain parametric regimes as shown by Berthomier et al. (2000), determining the effect of multi ion species in the plasma, and bringing the outputs of the model into the domain of the WBD measurements, i.e., ESW pulse electric field amplitude, and time duration. Previously, Dubouloz et al. (1991) had proposed that the high frequency part of the broadband spectrum that extended above the electron plasma frequency and observed on the Viking satellite in the dayside auroral zone could be the result of electron acoustic solitons passing by the satellite. Berthomier et al. (2003) also invoked the electron acoustic instability to explain the scaling of 3D solitary waves that were observed by FAST in the auroral acceleration region and by the Polar satellite over a wide range of altitudes from about 1 to 8 R_E. Although there is no observational evidence yet to suggest that 2D or 3D ESWs exist in the magnetosheath, a further refinement of our model to 2D or 3D might help in our interpretation of the observations. Based on the evidence for the acoustic instability being active in other regions of the magnetosphere and on our electron acoustic soliton model results presented above, there is every reason to believe that this instability may be active in the magnetosheath as well since we have shown that both cold and hot electrons, which are necessary for the acoustic instability (Singh and Lakhina, 2001), are present there.

There are some other generation mechanisms that show promise for generating the magnetosheath ESWs, however. Pickett et al. (2005) considered some other theories for the generation of these solitary waves which we will briefly mention. Foremost among these are the beam instabilities that have been invoked to explain the generation of ESWs in the magnetotail, auroral acceleration region, and cusp (e.g., Omura et al., 1996; Goldman et al., 1999; Singh et al., 2000; Newman et al., 2001; Tsurutani et al., 2003; Lakhina et al., 2004). These instabilities lead to holes in phase space (BGK solitary waves). Another theory that involves an electron beam was put forth by Jovanović and Shukla (2004). They proposed a model that is based on a drift-kinetic theory for electron phase space vortices in magnetized space plasmas. Their model involves the presence of an electron beam and is formulated in the frequency range of the lower hybrid waves excited by the Buneman instability. The electron holes that grow from this instability have the form of either elongated cylinders oblique to the magnetic field, or spheroids. Pickett et al. (2005) found that for most cases when ESWs are observed in the magnetosheath, counter-streaming electrons are observed, but they are not necessarily highly beamed. Nonetheless, these have the potential to create BGK solitary waves. We also mention the theoretical model of Fijalkow and Nocera (2004) of a hot collisionless plasma in a background of cold ions governed by the Vlasov–Poisson system of equations in one space and one velocity dimension. This study is particularly noteworthy because the simulations show that for sufficiently large values of the system's perturbation amplitude and sufficiently small values of the Landau damping rate, they observe the development of two streets of phase space holes each consisting of two counter-streaming families of holes. The two streets move in the phase space at different speeds and they may consist of a different number of holes. Perhaps this is the explanation for why Cluster often observes opposite polarity ESWs in the magnetosheath with similar time durations. In the Fijalkow and Nocera (2004) model, holes of the same street do not interact while those belonging to different streets do. Further, some holes become so large that they decay over time. Finally, there is the strong possibility of spontaneous generation of phase space holes out of the turbulence that is persistent throughout the magnetosheath as proposed by Chen et al. (2005). In their study of electron phase space holes, analyzed in terms of solitary wave solutions to the nonlinear Vlasov–Poisson equations in a collisionless plasma, they found that the width–amplitude relations for 1D and 3D electron holes are derived to be inequalities that allow the existence of the holes in regions on one side of a bound. They applied their theory to Polar data from the cusp and plasmasheet/plasmasheet boundary layer as published by Franz et al. (2005). They reported that electron phase space holes populate an allowed region in the solution space that is significantly away from the bounding curve. Thus, the results of Chen et al. (2005) show the accessibility of electron holes whose widths and amplitudes are only loosely constrained, thus opening up the possibility of spontaneous generation in a turbulent plasma even in the absence of two-stream or current-driven instabilities. All of the theories discussed above need to be explored for the magnetosheath region through simulations using inputs similar to those used above for the electron acoustic soliton model in order to better understand the physical processes that take place in the magnetosheath.

3. ESW propagation

3.1. In situ observations in the magnetosheath

Obtaining a measure of ESW velocity in space by observing propagation from one spacecraft to another is very difficult. Only one such case of observed propagation has thus far been published, that being for a pair of tripolar ESWs observed along auroral field lines at 4.8 R_E, $-36°$ λ_M and 22:09 MLT (Pickett et al., 2004b). The conclusion of that study was that the ESWs are evolving (growing, decaying) significantly in the time it takes to traverse from one spacecraft to another so that their shapes are unrecognizable or the ESWs have decayed before arriving at the second spacecraft. Complicating the measurements are several things: (1) the antennas must be about at the same angle to the background magnetic field or their shapes will probably look different on both spacecraft, (2) sometimes ESWs are seen close in time with oppositely directed initial polarities, indicating either ESWs traveling in opposite directions or ESWs with opposite polarities, with the former being the

most likely given that the pulse time durations are quite similar, (3) the ESWs could be traveling in the same direction but at different speeds, thus making it extremely difficult to cross correlate waveforms from two different spacecraft, (4) the ESWs may be coalescing as they propagate, (5) the spacecraft almost never lie along the same magnetic field line, or do not remain on the same field line long enough, (6) a mixture of modes in any one region leading to ESWs with characteristics different enough from each other that untangling them from one spacecraft is nearly impossible, and (7) the ESWs are almost all too small to be detected by a second spacecraft over such vast distances. Prior to the ESW propagation results reported in Pickett et al. (2004b), the only method for determining the velocity of ESWs was through interferometry techniques on a signal spacecraft (cf., Franz et al., 1998). This method will give a propagation observed over distances only as large as the two spacecraft antennas used to make the measurement, this being on the order of 100 m or less with delay times from one antenna to the next on the order of 50–100 μs. Thus, part of the reason for trying to identify ESW propagation over distances as large as the Cluster spacecraft separations, their smallest being on the order of a few 10s of km along the magnetic field and a few 100s km total separation, is to understand something about their stability, which will then help us to distinguish their mode.

We now present a case of ESW propagation observed in the magnetosheath from Cluster SC3 to SC4 when the spacecraft were at a location of about 11.85 R_E, −53.9° λ_M, and 13:32 MLT about an hour before they crossed the magnetopause and entered the cusp. Fig. 5 shows the following by panel: (a) waveform measurements obtained by SC3 over an 8 ms time period showing an offset bipolar pulse centered at about 2.75 ms and a usual bipolar pulse centered at about 5 ms, both with peak-to-peak amplitudes on the order of 0.4 mV/m, with time durations ~600 μs; (b) waveform measurements obtained by SC4 over an 8 ms time period showing an offset bipolar pulse centered at about 2.75 ms and usual bipolar pulse centered at about 5 ms, both of which have amplitudes >0.2 mV/m (waveforms are clipped due to insufficient digital resolution as opposed to receiver saturation) and time durations of ~600 μs, and several small amplitude bipolar pulses; (c) correlation coefficient vs. lag time of the SC3 measurements from those of SC4, showing the highest correlation of 0.55 at a lag of 22.5 ms; and (d) overplot of SC3 (green line) and SC4 (black line) waveforms incorporating the 22.5 ms lag of SC3 from SC4 and showing good agreement in amplitude and time for the two largest offset and usual bipolar pulses. The angle of the measuring antenna to the magnetic field for each of SC3 and SC4 are 45° and 20°, respectively, with the measured ESW pulses showing the same initial pulse polarities and similar pulse shapes as expected. At this time the spacecraft are separated ~30 km along **B** and 40 km perpendicular to **B**. The first conclusion we can draw from this analysis is that the lifetime of the ESWs in this region of space can be as great as 22.5 ms, and that they are stable over distances as great as 30 km. Based on the separation distances and the lag time, we calculate a velocity of these structures of 1334 km/s away from earth, with a size along the field of 0.8 km and a size cross field of at least 40 km. Thus, our second conclusion is that these structures are extremely pancake shaped, similar to those reported by Pickett et al. (2004b) to be propagating along auroral field lines from one Cluster spacecraft to another. Finally, we note that some of the smaller amplitude ESWs observed more prominently on SC4 seem to correlate with weak ESWs on SC3, yet some others do not correlate at all. Most of these smaller amplitude ESWs are near the noise floor of the receivers making it difficult to cross correlate the waveforms at these times or to state with certainty that they are ESWs. In addition there is the possibility as noted above that the smaller amplitude ESWs are damping out while traveling from one spacecraft to the other or are traveling at different speeds relative to the larger amplitude ones and thus not expected to correlate with the same lag time.

Our Cluster observations of flat structures (size along **B** much smaller than perpendicular) is consistent with the findings of Franz et al. (2000) who conclude that the electron holes observed by Polar are roughly spherical when the electron cyclotron frequency, Ω_e, is greater than the plasma frequency, ω_p, becoming more oblate ($L_\perp > L_\parallel$) with decreasing Ω_e/ω_p. Their scaling argument was based upon electron gyrokinetic theory. Berthomier et al. (2003) used a 3D fluid model of a 3D electron acoustic beam soliton to come to the same conclusion, i.e., that spheroidal potential structures will exist at FAST altitudes (below 4000 km), while at higher altitudes the solitary waves will be elongated across the magnetic field. Their results further suggested that the large amplitude solitary structures observed by the FAST and Polar satellites at different altitudes evolve from small amplitude electron acoustic solitons and are essentially 3D from the very beginning of their evolution. Finally, Volosevich et al. (2006) have developed a theoretical model of nonlinear electrostatic structures in space plasma based on an MHD system of equations for three-component plasmas, the evolutionary equations of which are the modified Kortweeg-deVries-Zakharov-Kuznetzov equations (KDV-ZK). They found that the structures will be spherical when the Larmor radius is much less than the Debye radius. When the Larmor radius is much greater than the Debye radius (it is not clear how an MHD-based formulation can address this regime), the perpendicular (to **B**) scale of the structure will be much more than the parallel (to **B**) scale, leading to almost flat structures. However, they concluded that electron acoustic structures should be more symmetric than ion acoustic structures. Since the case just presented here in Fig. 5 is the first to show propagation of ESWs in the magnetosheath, it will now be possible to more adequately test these various theories since we now have obtained properties such as velocity and size of ESWs in the magnetosheath.

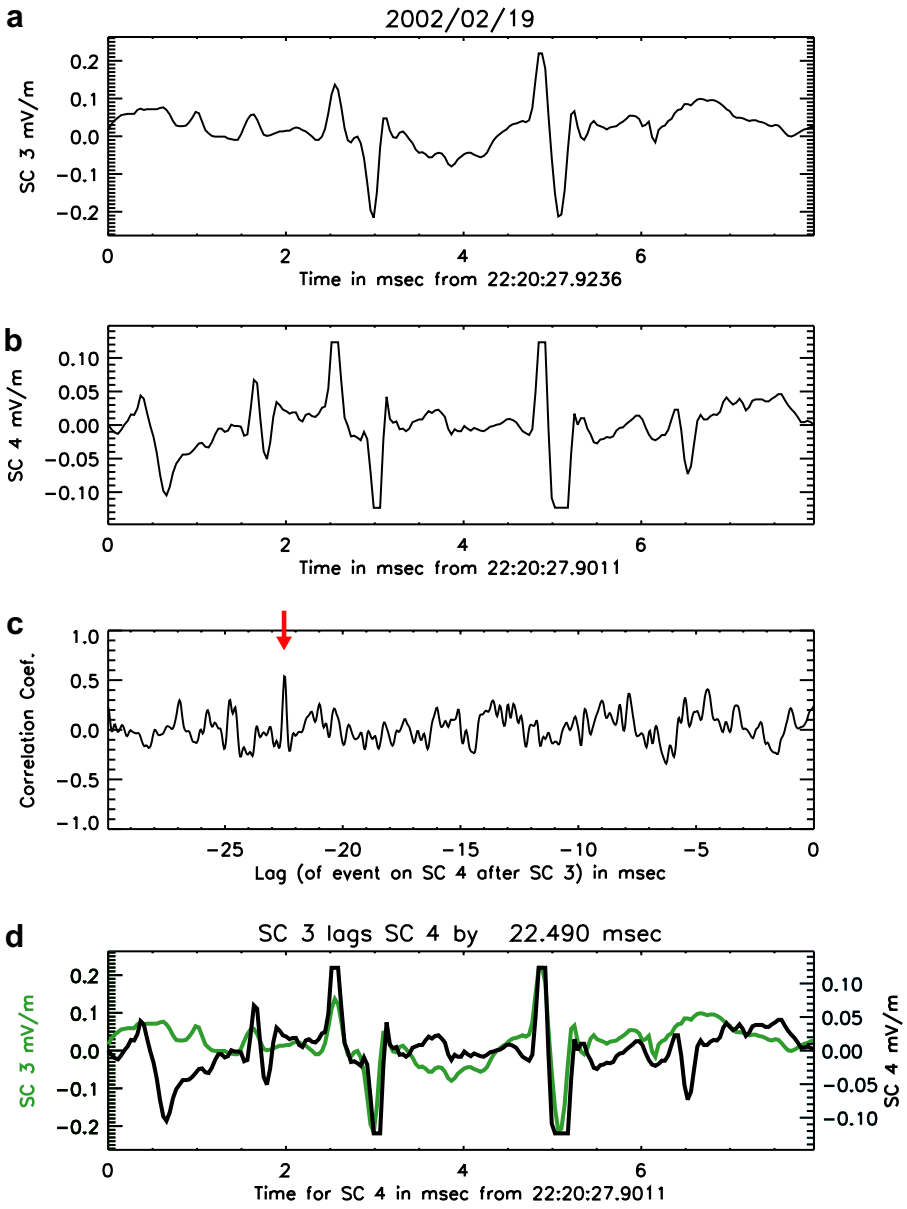

Fig. 5. ESW propagation from SC4 to SC3: (a) waveform from SC3 showing an offset bipolar pulse followed by a usual bipolar pulse, (b) waveform from SC4 showing the same primary bipolar pulses as in panel (a) plus several small amplitude pulses, (c) results of cross correlating the SC3 waveform with that of SC4, showing the best correlation of 0.55 at a lag of 22.5 ms of SC3 from SC4, and (d) overplot of SC4 and SC3 waveforms using the lag time of 22.5 ms providing confidence that the two major bipolar pulses observed on SC4 are the same ones observed on SC3 22.5 ms later.

3.2. Remote observations of ESW propagation in the auroral acceleration region

Using FAST spacecraft data, Pottelette et al. (2001) first reported that electron holes excited in the Auroral Kilometric Radiation (AKR) source region were the cause of the observed fine structure in AKR radiation. They demonstrated that a substantial part of the AKR emission consisted of a large number of elementary radiation events that were interpreted as travelling electron holes that may have resulted from the nonlinear evolution of electron acoustic waves and have the properties of BGK modes. In a follow-up study, Pottelette and Treumann (2005) provided evidence for electron holes in the upward current region, thus solidifying their earlier conclusion that the electron holes are responsible for the fine structure of AKR emissions. In the latter work, isolated parallel electric field structures of tripolar polarity were interpreted in terms of trains of nested ion and electron holes such as shown in the numerical simulations of Goldman et al. (2003). The tripolar structures are created by beam plasma interaction via the kinetic two-stream instability upstream of a strong double layer. Thus, began the era of using remote observations to observe the propagation of ESWs in the auroral acceleration region.

Recently, Mutel et al. (2006) reported that Cluster observes a specific type of fine structure AKR known as striped or striated AKR (SAKR) (Menietti et al., 1996, 2000) in about 1% of all WBD spectra when the spacecraft are located above 30° λ_M (plasmasphere shadowing prevents detection below that latitude). An example of the SAKR observed by the four Cluster spacecraft on 17 July 2002 is shown in the frequency time spectrogram of Fig. 6. In this figure we see several negative sloped SAKR traces in the frequency range 125.5–136 kHz (near the filter cut-off frequency) that correlate well on all four spacecraft. At this time the spacecraft separations were on the order of 8000 km and they were located in the nightside magnetosphere at about 11 R_E, −60° λ_M, and 04:00 MLT. By using multispacecraft measurements of the beaming pattern of SAKR bursts, Mutel et al. (2006) determined that the SAKR bursts are narrowly beamed, typically smaller than a 10° beam size. They used this beam size to estimate the intrinsic power of individual SAKR bursts, which were in the range 1–10 W, much smaller than previous estimates for certain types of fine-structured AKR (e.g., Pottelette et al., 2001). Mutel et al. (2006) have proposed that these SAKR bursts can be used as a remote sensor of ion holes and can thus be used to determine the frequency of occurrence, locations in the acceleration region, and lifetimes of those ion holes. They used the electric field signatures of ion holes observed in the upward current region to investigate the perturbation caused by the passage of an ion hole on a "horseshoe" electron velocity distribution in dilute plasma. They found that the cyclotron maser instability, which is believed to be the mechanism by which AKR is generated (cf., Treumann, 2006 for a recent review), is strongly enhanced inside the ion hole, with power gain exceeding 100 dB in a narrow frequency range just above the x-mode cut-off frequency. They thus compared the characteristics of ion holes measured in the upward current region (Bounds et al., 1999; Dombeck et al., 2001) to the characteristics of the structures represented by the SAKR bursts. They found very good agreement in terms of speed (75–400 km/s), direction of propagation (upward), and spacing of bursts (30–300 ms) where the observed frequency drift rate of SAKR, ranging between −2 and −8 kHz/s, and the SAKR bandwidth were used to obtain the ion hole speed and direction. Based on this good agreement and the possibility of ion holes to enhance the cyclotron maser instability, they concluded that SAKR bursts could be the tracers of ion holes propagating in the upward current region.

The primary new findings that Mutel et al. (2006) obtained from the analysis of SAKR are the following: (1) ion holes can propagate upward for more than 1000 km, implying lifetimes of a few seconds; (2) the ion holes propagate at nearly constant speed for their entire lifetime; (3) there is little evolution of the electric field intensity or spatial structure of ion holes over their lifetime; and (4) the ion holes are much more common at higher altitude with a 100 times higher probability of occurring at 10,000 km as opposed to 3200 km. Some numerical simulations show ion hole lifetimes of only about 5–75 ms and a significant change in ion hole speed as they evolve (Crumley et al., 2001), which is not observed (see 1 and 2 just above). However, these particle-in-cell simulations of soli-

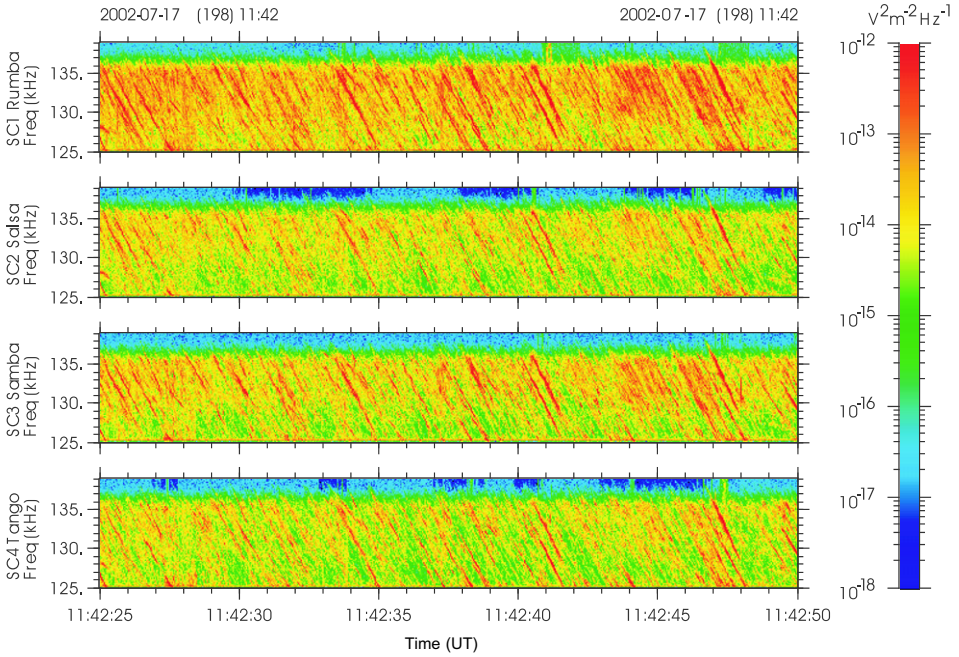

Fig. 6. Spectrogram of the waves observed on all four Cluster satellites on 17 July 2002 over a 25 s time interval in the frequency range of 125.5–136 kHz (the filter cut-off) showing striated Auroral Kilometric Radiation (negative sloped stripes persisting across much of the frequency range) that correlates well across all four satellites. These remotely sensed striations are thought to be tracers of ion holes propagating in the auroral acceleration region.

Table 1
Comparison of ESW characteristics obtained from single and multispacecraft observations and theory/simulation

	E-field (mV/m)	Time duration (ms)	Velocity (km/s)	Lifetime (ms)	$L_{\parallel}$ (km)	$L_{\perp}$ (km)
Auroral field lines/plasmasheet at 5–8 R_E (electron solitary waves)						
Single spacecraft interferometry (in situ)	1	0.5–1.0	500–2500	$\geqslant$0.08	0.1–1.0	>0.1–1.0
Multispacecraft (in situ)	0.2–3	0.5–1.0	900–2800	$\geqslant$20–22	0.7–4.5	>30–250
Theory/simulation	–	–	–	–	–	–
Magnetosheath						
Single spacecraft interferometry (in situ)	0.2–1.0	0.03–0.25	–	–	–	–
Multispacecraft (in situ)	0.1	0.075	1334	22.5	0.8	>40
Theory/simulation[a]	–	–	–	–	0.01–0.05	–
Auroral acceleration region (ion solitary waves)						
Single spacecraft interferometry (in situ)	10–500	3–10	75–300 at 5500–7000 km	$\geqslant$10	2–4	3–4
Multispacecraft (remote sensing)	>100	–	75–400	Few 1000	O(1)	–
Theory/simulation[b]	–	–	200–300	5–75	2	2

[a] Electron acoustic soliton model (Pickett et al., this paper).
[b] Simulations using a 2 spatial and 3 velocity dimension electrostatic code with one electron and two ion species (Crumley et al., 2001).

tary waves performed using a 2 spatial and 3 velocity dimension electrostatic code with one electron and two ion species need to be repeated with small time steps and spatial scales in order to see better how the spatial structure of ion solitary waves evolves. In addition He^{+} and hot plasma sheet ions need to be included since these populations are observed in the upward beam region.

4. Summary and conclusions

Above we have examined some of the characteristics and propagation of ESWs through in situ and remote observations on single and multiple satellites as well as through theory and simulation. In Table 1, we summarize these results and the results from some previous published works for three different regions: along Earth's auroral field lines at 5–8 R_E, (plasmasheet) for electron solitary waves, the magnetosheath (no distinction can be made as to whether these are ion or electron solitary waves), and the auroral acceleration region for ion solitary waves. The conclusions we draw from this table are the following: (1) multispacecraft observations provide additional information about the lifetime and stability of ESWs that go beyond those of single spacecraft observations; (2) spherical ESWs are observed primarily in the auroral acceleration region, while more oblate or flat ESWs are found in most other regions; (3) remote sensing of ESWs provides a powerful tool to help understand processes that occur in the auroral acceleration region; (4) there is much work still to be done on the theory and simulation side that will ultimately help us to better understand how ESWs are generated in various regions around Earth, other planets and in interplanetary space, and how they may influence the ongoing plasma processes in these regions.

Acknowledgements

We thank J. Swanner, J. Dowell, and J. Seeberger from The University of Iowa for the processing of the WBD data. We also thank C. Abramo, R. Parades, G. Hewitt, and all of the DSN staff for the superb scheduling and retrieval of the Cluster WBD data through DSN and the Cluster teams at ESTEC, ESOC, and JSOC who helped in facilitating the WBD measurements, which as we found out is a very complex and time consuming process. The authors from The University of Iowa acknowledge the support of NASA Goddard Spaceflight Center under Grant NNG04GB98G. G.S.L. thanks the Council of Scientific and Industrial Research (CSIR), Government of India, for the support under the Emeritus Scientist Scheme. The portion of the work performed by B.T.T. was done at the Jet Propulsion Laboratory under contract with NASA, California Institute of Technology.

References

Balogh, A., Dunlop, M.W., Cowley, S.W.H., Southwood, D.J., Thomlinson, J.G., et al. The Cluster magnetic field experiment. Space Sci. Rev. 79, 65–91, 1997.

Béghin, C., Décréau, P.M.E., Pickett, J., Sundkvist, D., Lefebvre, B. Modeling of Cluster's electric antennas in space: application to plasma diagnostics. Radio Sci. 40, RS6008, doi:10.1029/2005RS003264, 2005.

Berthomier, M., Pottelette, R., Malingre, M., Khotyaintsev, Y. Electron acoustic solitons in an electron-beam plasma system. Phys. Plasmas 7, 2987–2994, 2000.

Berthomier, M., Pottelette, R., Muschietti, L., Roth, I., Carlson, C.W. Scaling of 3D solitary waves observed by FAST and POLAR. Geophys. Res. Lett. 30, 2148, doi:10.1029/2003GL018491, 2003.

Bounds, S.R., Pfaff, R.F., Knowlton, S.F., Mozer, F.S., Temerin, M.A., Kletzing, C.A. Solitary potential structures associated with ion and electron beams near 1 R_E altitude. J. Geophys. Res. 104, 28709–28717, 1999.

Chen, L.-J., Pickett, J.S., Kintner, P., Franz, J., Gurnett, D. On the width–amplitude inequality of electron phase space holes. J. Geophys. Res. 110, A09211, doi:10.1029/2005JA011087, 2005.

Crumley, J.P., Cattell, C.A., Lysak, R.L., Dombeck, J.P. Studies of ion solitary waves using simulations including hydrogen and oxygen beams. J. Geophys. Res. 106, 6007–6015, 2001.

Dombeck, J., Cattell, J., Crumley, J., Peterson, W.K., Collin, H.L., Kletzing, C. Observed trends in auroral zone ion mode solitary wave structure characteristics using data from Polar. J. Geophys. Res. 106, 19013–19021, 2001.

Dubouloz, N., Pottelette, R., Malingre, M., Treumann, R.A. Generation of broadband electrostatic acoustic solitons. Geophys. Res. Lett. 18, 155–158, 1991.

Fijalkow, E., Nocera, L. Superposition of phase-space hole streets in Vlasov plasmas. J. Plasma Phys. 71 (part 4), 1–10, doi:10.1017/S0022377804003368, 2004.

Franz, J.R., Kintner, P.M., Pickett, J.S. POLAR observations of coherent electric field structures. Geophys. Res. Lett. 25, 1277–1280, 1998.

Franz, J.R., Kintner, P.M., Seyler, C.E., Pickett, J.S., Scudder, J.D. On the perpendicular scale of electron phase-space holes. Geophys. Res. Lett. 27, 169–172, 2000.

Franz, J.R., Kintner, P.M., Pickett, J.S., Chen, L.-J. Properties of small-amplitude electron phase-space holes observed by Polar. J. Geophys. Res. 110, A09212, doi:10.1029/2005JA011095, 2005.

Goldman, M.V., Oppenheim, M.M., Newman, D.L. Nonlinear two-stream instabilities as an explanation for auroral bipolar wave signatures. Geophys. Res. Lett. 26, 1821–1824, 1999.

Goldman, M.V., Newman, D.L., Ergun, R.E. Phase-space holes due to electron and ion beams accelerated by a current-driven potential ramp. Nonlinear Proc. Geophys. 10, 37–44, 2003.

Gurnett, D.A., Huff, R.L., Kirchner, D.L. The wide-band plasma wave investigation. Space Sci. Rev. 79, 195–208, 1997.

Johnstone, A.D., Alsop, C., Burge, S., Carter, P.J., Coates, A.J., Coker, A.J., et al. PEACE: a plasma electron and current experiment. Space Sci. Rev. 79, 351–398, 1997.

Jovanović, D., Shukla, P.K. Solitary waves in the Earth's magnetosphere: nonlinear stage of the lower-hybrid Buneman instability. Geophys. Res. Lett. 31, L05805, doi:10.1029/2003GL018047, 2004.

Lakhina, G.S., Tsurutani, B.T., Kojima, H., Matsumoto, H. "Broad-band" plasma waves in the boundary layers. J. Geophys. Res. 105, 27791–27831, 2000.

Lakhina, G.S., Tsurutani, B.T., Pickett, J.S. Association of Alfven waves and proton cyclotron waves with electrostatic bipolar pulses: magnetic hole events observed by Polar. Nonlinear Proc. Geophys. 11, 205–213, 2004.

Menietti, J.D., Wong, H.K., Kurth, W.S., Gurnett, D.A., Granroth, L.J., Groene, J.B. Discrete, stimulated auroral kilometric radiation observed in the Galileo and DE1 wideband data. J. Geophys. Res. 101, 10673–10680, 1996.

Menietti, J.D., Persoon, A.M., Pickett, J.S., Gurnett, D.A. Statistical study of auroral kilometric radiation fine structure striations observed by Polar. J. Geophys. Res. 105, 18857–18866, 2000.

Mutel, R.L., Menietti, J.D., Christopher, I.W., Gurnett, D.A., Cook, J.M. Striated auroral kilometric radiation emission: a remote tracer of ion solitary structures. J. Geophys. Res. 111, A10203, doi:10.1029/2006JA011660, 2006.

Newman, D.L., Goldman, M.V., Ergun, R.E., Mangeney, A. Formation of double layers and electron holes in a current-driven space plasma. Phys. Rev. Lett. 85 (25), 1–4 (Art. No. 255001), 2001.

Omura, Y., Matsumoto, H., Miyake, T., Kojima, H. Electron beam instabilities as generation mechanism of electrostatic solitary waves in the magnetotail. J. Geophys. Res. 101, 2685–2697, 1996.

Pickett, J.S., Menietti, J.D., Gurnett, D.A., Tsurutani, B., Kintner, P.M., Klatt, E., Balogh, A. Solitary potential structures observed in the magnetosheath by the Cluster spacecraft. Nonlinear Proc. Geophys. 10, 3–11, 2003.

Pickett, J.S., Chen, L.-J., Kahler, S.W., Santolík, O., Gurnett, D.A., et al. Isolated electrostatic structures observed throughout the Cluster orbit: relationship to magnetic field strength. Ann. Geophys. 22, 2515–2523, 2004a.

Pickett, J.S., Kahler, S.W., Chen, L.-J., Huff, R.L., Santolík, O., et al. Solitary waves observed in the auroral zone: the Cluster multi-spacecraft perspective. Nonlinear Proc. Geophys. 11, 183–196, 2004b.

Pickett, J.S., Chen, L.-J., Kahler, S.W., Santolík, O., Goldstein, M.L., et al. On the generation of solitary waves observed by Cluster in the near-Earth magnetosheath. Nonlinear Proc. Geophys. 12, 181–193, 2005.

Pottelette, R., Treumann, R., Berthomier, M. Auroral plasma turbulence and the cause of the auroral kilometric radiation fine structure. J. Geophys. Res. 106, 8465–8476, 2001.

Pottelette, R., Treumann, R.A. Electron holes in the auroral upward current region. Geophys. Res. Lett. 32, L12104, doi:10.1029/2005GL022547, 2005.

Rème, H., Aoustin, C., Bosqued, J.M., Dandouras, J., Lavraud, B., et al. First multispacecraft ion measurements in and near the Earth's magnetosphere with the identical Cluster ion spectrometry (CIS) experiment. Ann. Geophys. 19, 1303–1354, 2001.

Singh, N., Loo, S.M., Wells, B.E., Deverapalli, C. Three-dimensional structure of electron holes driven by an electron beam. Geophys. Res. Lett. 27, 2469–2472, 2000.

Singh, S.V., Lakhina, G.S. Generation of electron-acoustic waves in the magnetosphere. Planet. Space Sci. 49, 107–114, 2001.

Singh, S.V., Reddy, R.V., Lakhina, G.S. Broadband electrostatic noise due to nonlinear electron-acoustic waves. Adv. Space Res. 28, 1643–1648, 2001.

Singh, S.V., Lakhina, G.S. Electron acoustic solitary waves with non-thermal distribution of electrons. Nonlinear Proc. Geophys. 11, 275–279, 2004.

Treumann, R.A. The electron-cyclotron maser for astrophysical application. Astron. Astrophys. Rev. 13, 229–315, 2006.

Tsurutani, B.T., Arballo, J.K., Lakhina, G.S., Ho, C.M., Buti, B., Pickett, J.S., Gurnett, D.A. Plasma waves in the dayside polar cap boundary layer: bipolar and monopolar electric pulses and whistler mode waves. Geophys. Res. Lett. 25, 4117–4120, 1998.

Tsurutani, B.T., Dasgupta, B., Arballo, J.K., Lakhina, G.S., Pickett, J.S. Magnetic field turbulence, electron heating, magnetic holes, proton cyclotron waves, and the onsets of bipolar pulse (electron hole) events: a possible unifying scenario. Nonlinear Proc. Geophys. 21, 27–35, 2003.

Volosevich, A.V., Meister, C.-V., Zhestkov, S.V. Theoretical model and experimental diagnostics of nonlinear electrostatic structures in space plasma. Adv. Space Res. 37, 569–575, 2006.

Williams, J.D., Chen, L.-J., Kurth, W.S., Gurnett, D.A., Dougherty, M.K., Rymer, A.M. Electrostatic solitary structures associated with the November 10, 2003 interplanetary shock at 8.7 a.u.. Geophys. Res. Lett. 32, L17103, doi:10.1029/2005GL023079, 2005.

Williams, J.D., Chen, L.-J., Kurth, W.S., Gurnett, D.A., Dougherty, M.K. Electrostatic solitary structures observed at Saturn. Geophys. Res. Lett. 33, L06103, doi:10.1029/2005GL024532, 2006.